Negative Surges in Open Channels: Physical and Numerical Modeling

Martina Reichstetter[1] and Hubert Chanson[2]

Abstract: Negative surges can be caused by a sudden change in flow resulting from a decrease in water depth. In the present study, some physical experiments were conducted in a rectangular channel to characterize the unsteady free-surface profile and longitudinal velocity beneath a negative surge propagating upstream. The physical observations showed that, during the first initial instants, the celerity of the surge leading edge increased rapidly with time, while later the negative surge propagated upstream in a more gradual manner with a celerity decreasing slowly with increasing distance. The velocity data highlighted some relatively large turbulent fluctuations beneath the negative surge. The physical results were used to test the analytical solution of the Saint-Venant equations and some numerical models. The findings suggested that the negative surge propagation appeared relatively little affected by the boundary friction within the investigated flow conditions. **DOI: 10.1061/(ASCE)HY.1943-7900.0000674.**

CE Database subject headings: Storm surges; Open channel flow; Unsteady flow; Numerical models; Velocity.

Author keywords: Negative surges; Unsteady open channel flow; Physical modeling; Numerical modeling; Water depth; Velocity; Negative waves.

Introduction

A negative surge is an unsteady open channel flow motion characterized by a decrease with time of the flow depth (Jaeger 1956; Henderson 1966; Montes 1998). Negative surges may occur downstream of a control structure when the discharge is reduced or upstream of a gate that is opened suddenly. For a stationary observer, the negative surge appears to be a gentle lowering of the free surface (Fig. 1).

A negative surge may be solved using the one-dimensional unsteady open channel flow equations called the Saint-Venant equations:

$$B\frac{\partial d}{\partial t}+\frac{\partial Q}{\partial x}=0 \tag{1}$$

$$\frac{\partial V}{\partial t}+V\frac{\partial V}{\partial x}=-g\frac{\partial d}{\partial x}+g(S_o-S_f) \tag{2}$$

where d and V = water depth and flow velocity, respectively; x = longitudinal coordinate positive downstream; B = free-surface width; g = gravitational acceleration; S_o = bed slope; and S_f = friction slope (Montes 1998; Chanson 2004). When the initial flow conditions (d_o, V_o) are constant along a channel, and $S_o = S_f$ at any time and space, the solution called simple wave solution yields the velocity and flow depth at any point (x, t) along a characteristic line as functions of the initial flow properties (V_o, d_o) and the flow depth d_1 at $x = x_{\text{Gate}}$ for $t = t_1$ [Fig. 1(b)]:

$$V=V_o+2\left(\sqrt{gd_o}-\sqrt{gd_1}\right) \qquad x_s<x<x_{\text{Gate}} \tag{3}$$

$$d=d_1 \tag{4}$$

Eqs. (3) and (4) provide the complete simple wave solution when the boundary condition is the time variations of water depth at the gate ($x = x_{\text{Gate}}$). Because $d_1 < d_o$, Eq. (3) implies a flow acceleration. The instantaneous longitudinal profile may be derived from the equation of the characteristics D-F issued from the gate:

$$x_{\text{Gate}}-x=\left(3\sqrt{gd}-2\sqrt{gd_o}-V_o\right)(t-t_1) \qquad x_s<x<x_{\text{Gate}} \tag{5}$$

which is a parabola. The negative surge propagates upstream at a celerity,

$$U=\sqrt{gd_o}-V_o \tag{6}$$

in a rectangular channel with U being the celerity positive upstream (Montes 1998; Chanson 2004). The characteristic diagram forms a series of diverging lines for a negative surge generated by the rapid opening of a downstream gate as illustrated in Fig. 1(a).

To date, the knowledge of the hydraulics of negative surges in open channels remains limited despite the classical experiments of Favre (1935) and some well-detailed presentations in textbooks (Montes 1998; Sturm 2001; Chanson 2004). The present study investigates physically and numerically the unsteady flow properties of negative surges against an initially steady flow. Some basic physical modeling was performed including free-surface and unsteady velocity measurements together with surge celerity observations. Both one-dimensional and two-dimensional modeling results are compared with the physical data. It is the aim of this work to characterize the propagation of negative surges against an initially steady open channel flow motion and to check the appropriateness of simple analytical and numerical models.

[1]Graduate Student, The Univ. of Queensland, School of Civil Engineering, Brisbane QLD 4072, Australia.

[2]Professor in Hydraulic Engineering, The Univ. of Queensland, School of Civil Engineering, Brisbane QLD 4072, Australia (corresponding author). E-mail: h.chanson@uq.edu.au

Note. This manuscript was submitted on November 2, 2011; approved on September 5, 2012; published online on September 6, 2012. Discussion period open until August 1, 2013; separate discussions must be submitted for individual papers. This technical note is part of the ***Journal of Hydraulic Engineering***, Vol. 139, No. 3, March 1, 2013. © ASCE, ISSN 0733-9429/2013/3-341-346/$25.00.

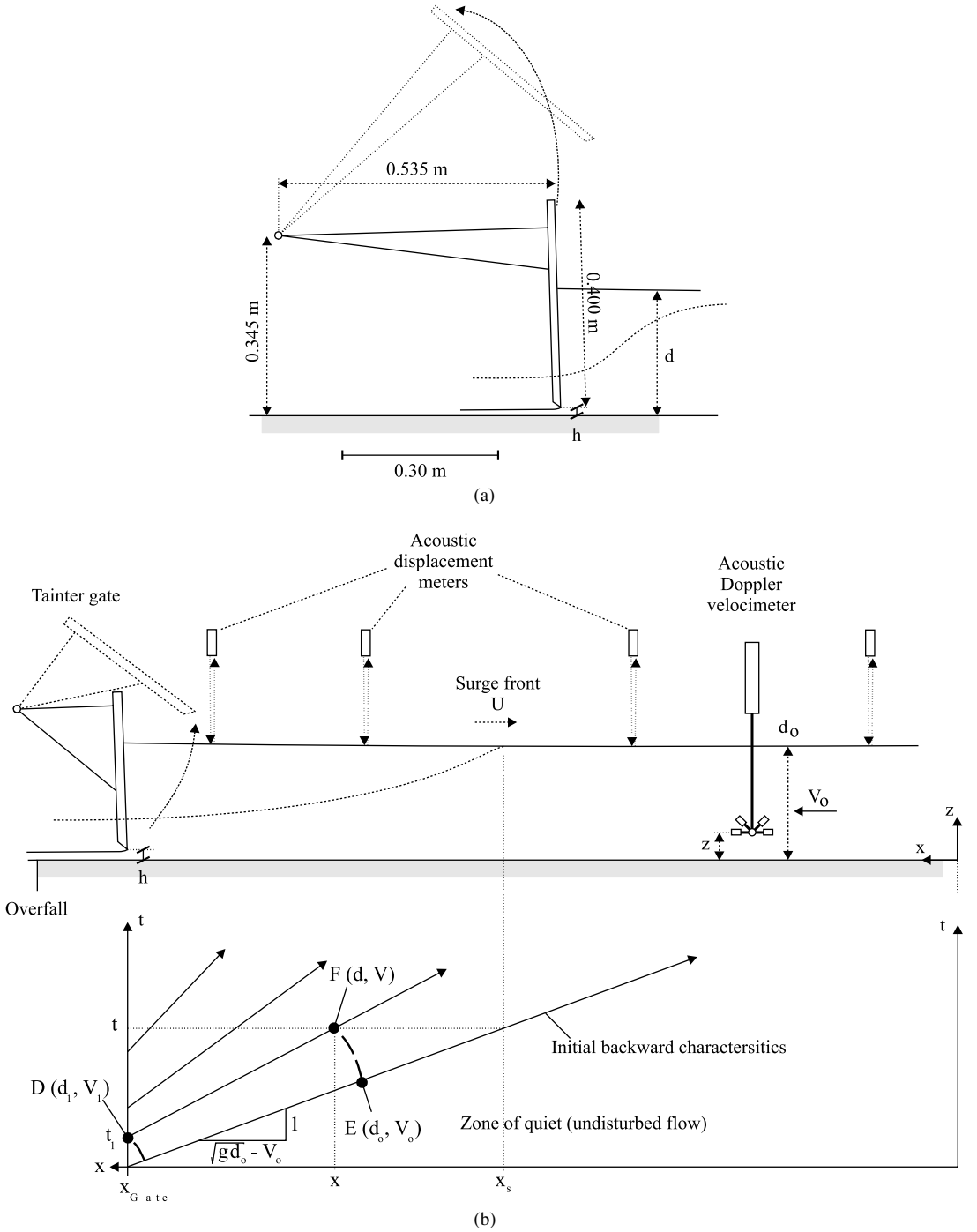

Fig. 1. Sketch of the negative surge propagating upstream and characteristic diagram for the simple wave solution (not drawn to scale) including details of the tainter gate; (a) dimensioned undistorted sketch of the tainter gate; (b) sketch of the negative surge propagating upstream

Physical Investigation of Negative Surges

The experiments were performed in a 12 m long, 0.5 m wide horizontal flume (Figs. 1 and 2). The channel was made of smooth polyvinyl chloride (PVC) bed and glass walls. The water was supplied by a constant head tank to a large intake chamber with a smooth convergent feeding into the glass-walled channel. A fast-opening gate was located at the channel downstream end, $x = 11.15$ m with $x = 0$ the channel upstream end [Fig. 1(a)].

The water discharge was measured with two orifice meters designed based on BS 1042:1943 (British Standard Institution 1943). The percentage of error was less than 2%. In steady flows, the water depths were measured using rail-mounted pointer gauges. The unsteady water depth was measured using a series of acoustic displacement meters, Microsonic Mic+25/IU/TC. The data accuracy and response of the displacement meters were 0.18 mm and 50 ms, respectively (Microsonic 2012). The instantaneous velocity components were measured using an acoustic Doppler velocimeter (ADV), Nortek Vectrino+equipped with a side-looking head. The velocity range was set to 1.0 m/s and the sampling rate was 200 Hz, while the data accuracy was 0.01 m/s (Nortek 2009). The translation of the ADV probe in the vertical direction was

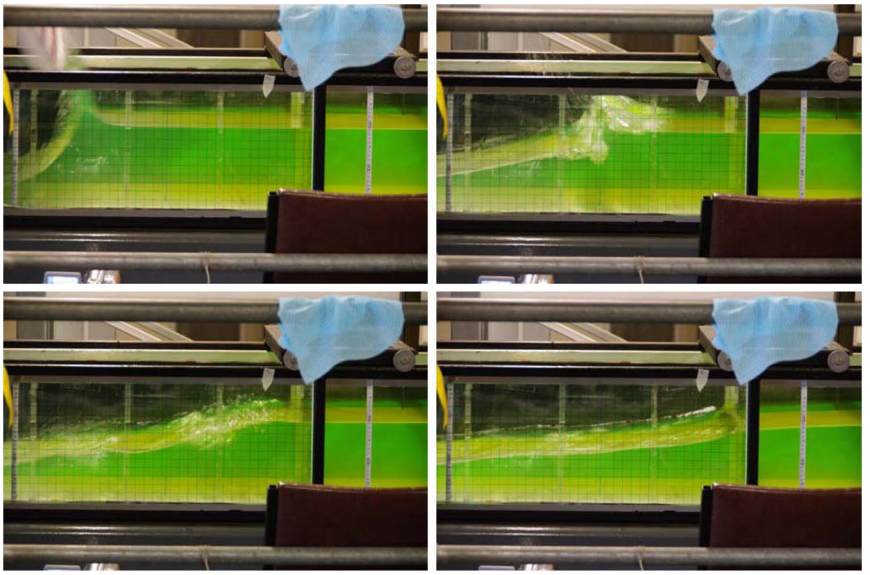

(a)

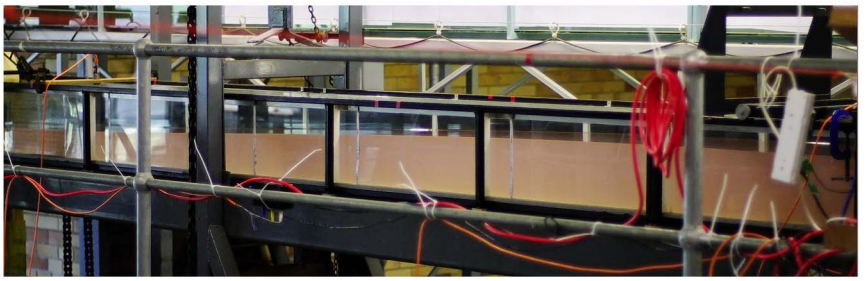

(b)

Fig. 2. Photographs of the negative surge experiments; (a) negative surge generation next to the gate: initial flow conditions were $Q = 0.020$ m^3/s, $h = 0$; photographs are after lens distortion corrections; clockwise from top left, $t = 0$, 0.19, 0.385, 0.577 s; the photograph covers 11.15 m $> x >$ 10.2 m, and the gate is on the far left-hand side; (b) negative surge propagating upstream: initial flow conditions were $Q = 0.020$ m^3/s (from right to left), $h = 0.030$ m; the photograph covers 11 m $> x >$ 7 m, and the gate is fully opened (left-hand side)

controlled by a fine adjustment traveling mechanism with an error less than 0.1 mm. All the measurements were taken on the channel centerline.

Two types of ADV postprocessing techniques were used. In steady flows, communication errors, average signal-to-noise ratio data less than 5 dB, and average correlation values less than 60% were removed, and the phase-space thresholding technique developed by Goring and Nikora (2002) and extended by Wahl (2003) was applied to remove spurious points in the ADV steady flow data set. The previously mentioned postprocessing techniques do not apply in unsteady flow conditions (Koch and Chanson 2009; Docherty and Chanson 2012). Thus, the unsteady flow postprocessing was limited to the removal of communication errors, although it was noted that the vertical velocity component V_z of data may be affected adversely by the bed proximity (Chanson et al. 2007; Chanson 2010).

A video camera, PanasonicNV-H30 (25 frames per second), was used to record the instantaneous free-surface profile at two different locations along the channel. A 20 mm squared grid was placed on the side wall for reference and lens distortion correction (Fig. 2). The focal plane of the camera was placed slightly beneath the initial free surface for the recorded image to show the free surface close to the wall rather than on the channel centerline. Additional information was recorded with a Pentax K-7 camera with a 14 Mp resolution. Further details are reported in Reichstetter and Chanson (2011).

Inflow Conditions and Negative Surge Generation

For each run, the steady gradually varied flow conditions were established prior to the measurements. The negative surge was produced by opening rapidly the tainter gate [Fig. 1(b)]. Its opening times were less than 0.15 to 0.2 s, which were small enough to have a negligible effect on the surge propagation (Lauber 1997). After the rapid opening, the gate did not intrude into the flow [Fig. 2(a)]. The experimental flow conditions are summarized in Table 1 in which Q is the initially steady flow rate, d_o and V_o are the initial flow depth and velocity recorded at $x = 6$ m, and h is the undershoot gate height before opening.

During the unsteady flow experiments, the displacement meters were located at $x = 5.6$, 6.0, 6.2, 10.2, 10.5, and 10.8 m. The video camera was centered either at $x = 6.0$ m covering $5.8 < x < 6.3$ m, or $x = 10.8$ m covering $10.5 < x < 11.2$ m (including the gate). The instantaneous velocity measurements were conducted for one series of flow conditions at $x = 10.5$ m and 6 m for four vertical elevations, $z = 0.0067$, 0.025, 0.124, and 0.135 m, where z is the elevation above the bed (Table 1). At each sampling location, the experiments were repeated several times to ascertain the experimental repeatability.

Table 1. Experimental Investigations of Negative Surges

Reference	S_o	Q (m^3/s)	h (m)	d_o (at $x = 6$ m) (m)	V_o (at $x = 6$ m) (m/s)	U (at $x = 6$ m) (m/s)	Instrument(s)
(1)	(2)	(3)	(4)	(5)	(6)	(7)	(8)
20–30 mm	0	0.020	0.030	0.24	0.17	0.91	Video, ADV, displacement meters
20–50 mm		0.020	0.050	0.10	0.40	0.25	Video
30–40 mm		0.030	0.040	0.26	0.23	0.33	Video
30–50 mm		0.030	0.050	0.22	0.27	0.49	Video

Note: h = undershoot gate height before sudden opening.

Physical Observations

Both visual observations and water-surface profile measurements showed a fast drop in water depth close to the gate (e.g., $10 < x < 11.15$ m) compared with the observations further upstream at $5.5 < x < 6.5$ m. Fig. 2 presents some photographs of the upstream propagation of negative surges. Fig. 2(a) shows four photographs of the surge generation immediately upstream of the gate within 0.8 s. The observations highlighted the rapid gate opening and surge formation. Very rapidly (within a second), any disturbance vanished and the instantaneous free surface exhibited a smooth shape as shown in Fig. 2(b). Fig. 2(b) presents an instantaneous shot of the water surface between $x = 7$ and 11 m. The present observations indicated some free-surface curvature immediately after the gate opening, typically for $t\sqrt{g/d_o} < 1.5$ [Fig. 2(a)]. For larger times, the free surface was very flat and smooth [Fig. 2(b)]. The water surface curvature was not discernable by eye and it is believed that the assumption of hydrostatic pressure was valid.

The celerity of the negative surge leading edge was deduced from photographic, video, and acoustic displacement meter measurements. The results are presented in Fig. 3 with the dimensionless surge celerity as a function of the longitudinal distance x/L, where L is the channel length ($L = 12$ m). In Fig. 3, the downstream gate is shown with a thick dashed line. For the investigated flow conditions (Table 1), the celerity data highlighted two distinct phases. Very close to the gate immediately after gate opening, the negative surge formation was associated with some local dissipative process [Fig. 2(a)]. During this formation phase, the celerity of the negative surge leading edge increased rapidly with time. The present data sets suggested that the acceleration phase took place within a distance 4 d_o from the gate. Afterward, the negative surge propagated upstream in a more gradual manner. The leading edge was very flat and barely perceptible, and its celerity tended to decrease slowly with increasing distance from the gate (Fig. 3, $x/d_o < 40$). At $x = 6$ m, the dimensionless surge celerity $(U + V_o)/(gd_o)^{1/2}$ ranged from 0.3 up to 1.0 depending on the initial steady flow conditions (Table 1).

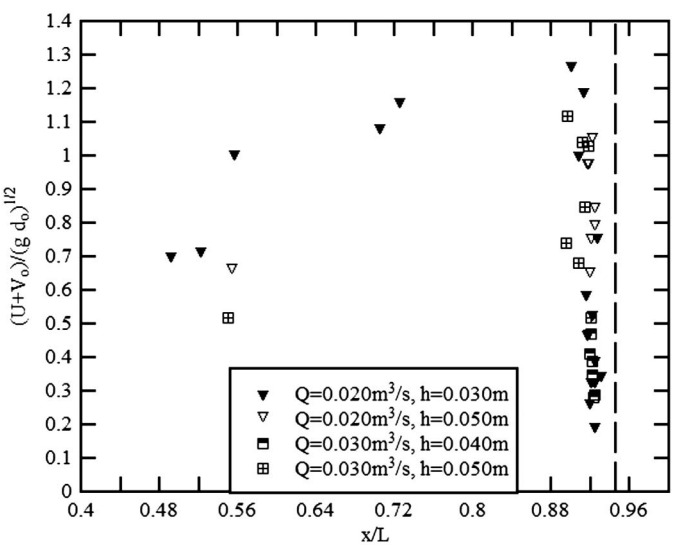

Fig. 3. Dimensionless negative surge celerity as a function of the longitudinal distance; surge propagation is shown from right to left

For comparison, the simple wave solution of the Saint-Venant equations predicts a constant dimensionless celerity $(U + V_o)/(gd_o)^{1/2} = 1$ [Eq. (6)]. In a rectangular flume, Favre (1935) measured the surge celerity propagating downstream as $(U + V_o)/(gd_o)^{1/2} = 1$. Tan and Chu (2009) reanalyzed the data set of Lauber and Hager (1998) in a 3.5 m long horizontal rectangular channel initially at rest ($V_o = 0$), and their computational data matched the experimental observations: $U/(gd_o)^{1/2} = 1$. The present results (Fig. 3, Table 1) suggest that neither the Saint-Venant equations solution nor previous findings were comparable with the present results. In this research, the gradually varied phase was associated with some slight deceleration of the negative surge leading edge. The gradual deceleration of the surge leading edge might be possibly linked with the initial (nonstill) flow conditions as well as the upstream surge propagation against an H2 backwater profile with very slight changes in depth with increasing distance from the gate. That is, the free-surface and velocity measurements in steady flows implied that the flume was hydraulically smooth. It is believed that the upstream propagation of the negative surge against the initially steady flow was associated with some turbulence dissipation throughout the water column, evidenced by the relatively high turbulent velocity fluctuations during the surge propagation. The transient turbulent dissipation process might be responsible for some gradual deceleration of the surge leading edge.

During the negative surge, the water depth decreased relatively gradually after the initial surge formation. The free-surface measurements showed some curvature near the surge leading edge (Fig. 4). Fig. 4 presents some typical free-surface measurements close to the gate ($x = 10.8$ m) and further upstream ($x = 6$ m). The upstream propagation of the surge was associated with an increase in longitudinal velocity (Fig. 5). Fig. 5 includes some typical instantaneous velocity measurements at $x = 6$ m for two vertical elevations. At $x = 6$ m, the velocity data showed some relatively large fluctuations during the initial phases of the surge propagation, compared with the steady-state data. For example, at $t(g/d_o)^{1/2} \sim 20$ in Fig. 5, the turbulent velocity fluctuations about the smoothed data trend were nearly 2.5 times larger than in the initially steady flow. Further, during the drawdown of the free surface [$21 < t(g/d_o)^{1/2} < 45$], the velocity fluctuations were on average 1.5 times larger than those in the initially steady flow. The increase in turbulence observed during the negative surge propagation including at the leading edge might suggest some enhanced turbulent mixing.

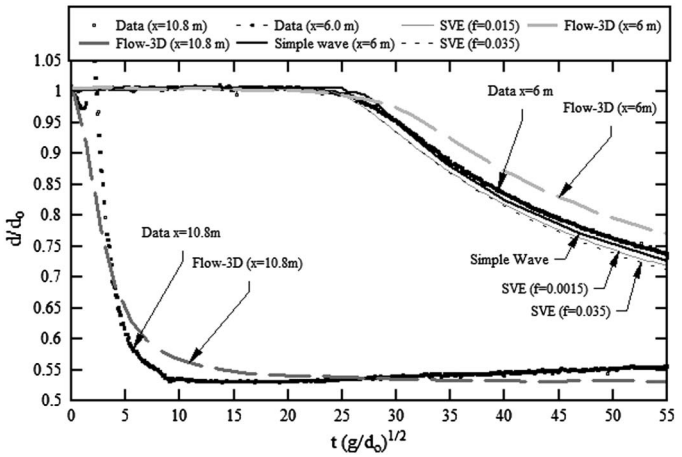

Fig. 4. Dimensionless time variations of water depth beneath a negative surge: comparison between physical data at $x = 10.8$ and 6.0 m, analytical calculations, and numerical results (Saint-Venant equations and Flow-3D); flow conditions were $Q = 0.020$ m^3/s, $h = 0.030$ m, and $d_o = 0.24$ m

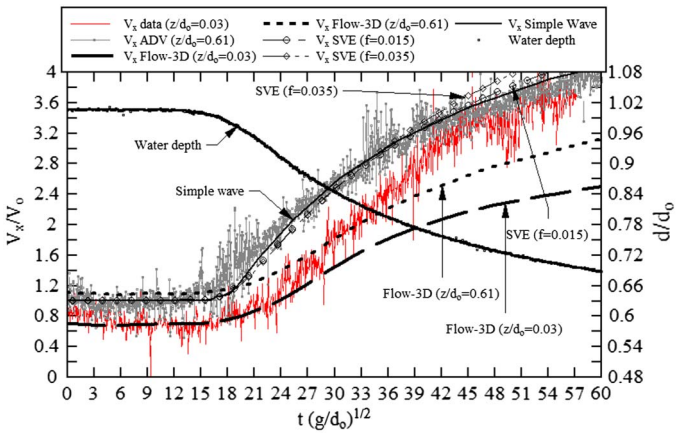

Fig. 5. Dimensionless time variations of water depth and longitudinal velocity beneath a negative surge: comparison between physical data at $x = 6.0$ m ($z/d_o = 0.030$ and 0.615), analytical calculations, and numerical results (Saint-Venant equations and Flow-3D); flow conditionswere $Q = 0.020$ m^3/s, $h = 0.030$ m, and $d_o = 0.24$ m

Comparison with Analytical and Numerical Models

The physical data set was used to test three models of the negative surge: an analytical model and two numerical models (Table 2). The first model (M1) was an analytical solution of the Saint-Venant equations based on the simple wave approximation [Eqs. (3–6)]. The second model (M2) was a numerical integration of Saint-Venant equations using the Hartree method (Courant et al. 1952; Montes 1998). The one-dimensional solution was integrated from $x = 10.8$ m using the measured flow depth for its downstream boundary condition. The last model (M3) was a two-dimensional numerical model (vertical plane corresponding to the channel centreline) using the software Flow-3D. The classic re-normalisation group (RNG) turbulence model was selected for its robustness, and a 5 mm uniform mesh size was used (Table 2). The downstream boundary condition was a sudden gate removal with a translational vertical velocity of +1 m/s. Further details on the computational fluid dynamics (CFD) modeling were reported in Reichstetter and Chanson (2011).

The analytical solution and numerical model data were compared with the free-surface physical data (Fig. 4). Fig. 4 presents the comparative results in terms of the free-surface data at $x = 6$ and 10.8 m. The simple wave solution with no friction compared well with the physical measurements, and this is consistent with the hydraulically smooth flume. The CFD results were close to the physical observations at $x = 10.8$ m, but the water depth predictions at $x = 6$ m were consistently higher than the observations (Fig. 4). This might be a result of different downstream boundary conditions, i.e., an idealized gate removal for the CFD versus the measured data at $x = 10.8$ m (immediately upstream of the gate) for the integration of Saint-Venant equations.

Some comparative results in terms of longitudinal velocity data are presented in Fig. 5, showing the physical data at two elevations, the one-dimensional calculations based on the simple wave method and Saint-Venant equation integration, and the two-dimensional CFD results. The simple wave and Saint-Venant equation results were depth-averaged velocity data. The analytical and numerical results compared qualitatively well with the experimental measurements. All the data highlighted the flow acceleration beneath the negative surge. Both the physical observations and CFD results indicated an increase in longitudinal velocity components with increasing vertical elevation at a given time. However, neither the analytical nor numerical solutions could reproduce the turbulent fluctuations around the mean trend. The CFD results generally underestimated the longitudinal velocities beneath the negative surge at all vertical elevations.

In general, the simple wave method compared well with the experimental data, and it was the least time-consuming method. Both the simple wave method and Saint-Venant equation integration required an initial input time series (water depth) for the downstream boundary to predict the surge propagation.

Conclusion

In the present study, new physical experiments were conducted in a relatively large rectangular channel to characterize a negative surge

Table 2. Summary of Analytical and Numerical Models of the Negative Surge

Model	Type	Description	Details	Downstream boundary conditions	Flow conditions
(1)	(2)	(3)	(4)	(5)	(6)
M1	Analytical	Simple wave	—	Measured depth at $x = 10.8$ m	$Q = 0.020$ m^3/s, $h = 0.030$ m
M2	Numerical (one-dimensional)	Integration of Saint-Venant equations	Hartree method ($\Delta x = 0.1$ m, $\Delta t = 0.05$ s), $f = 0.015$ to 0.035	Measured depth at $x = 10.8$ m	
M3	Numerical (two-dimensional)	Flow-3D (version 9.3)	Uniform mesh size: 5, 15, 30 mm, RNG turbulence model	Sudden gate removal (vertical motion, +1 m/s)	

propagating upstream against an initially steady flow. Some velocity measurements were performed using ADV, while the free-surface elevations were recorded using nonintrusive techniques. The physical results were used as benchmarks to test some analytical and numerical models. The physical observations showed that, during the first initial instants following gate opening (formation phase), the celerity of the negative surge leading edge increased rapidly with time up to $x_{Gate} - x = 4d_o$. Afterward, the negative surge propagated upstream in a more gradual manner: the surge leading edge was very flat and the celerity tended to decrease slowly with increasing distance from the gate. The rate of water elevation decrease was the largest at the beginning of negative surge propagation, when the longitudinal velocity increased during the initial stages of negative surge. The velocity data highlighted some increased turbulence beneath the negative surge with relatively large velocity fluctuations. The physical results were used to test the analytical solution of the Saint-Venant equations and some one- and two-dimensional numerical results. The findings suggested that the negative surge propagation was relatively little affected by the boundary friction within the investigated flow conditions. For the relatively simple geometry, in this paper a prismatic rectangular flume, the physical data were modeled well by the simple wave analytical solution. Both numerical model results were qualitatively in agreement with the experimental observations.

The present results suggested that the negative surge remains a challenging topic for the computational modellers.

Acknowledgments

The authors thank Graham Illidge, Clive Booth, and Ahmed Ibrahim (The University of Queensland) for their technical assistance. They thank further Dr. Luke Toombes (Aurecon) for his valuable advice and inputs. The assistance of Prof. Peter Rutschmann (Technical University of Munich) to perform the CFD modeling is acknowledged. The authors acknowledge the helpful comments of Prof. Fabian Bombardelli (UC Davis), Prof. John Fenton (Technical University of Vienna), and Dr. Pierre Lubin (University of Bordeaux). The financial support of the Australian Research Council (Grant DP120100481) is acknowledged.

Notation

The following symbols are used in this paper:

A = flow cross-section area (m^2);
B = channel width (m);
C = celerity (m/s) of a small disturbance in shallow water: $C = \sqrt{gd}$ in a rectangular channel;
d = water depth (m) measured above the invert;
d_1 = characteristic depth (m) at $x = x_{Gate}$ and $t = t_1$;
F = Froude number locally defined as $\mathsf{F} = V/\sqrt{gd}$;
f = Darcy-Weisbach friction factor;
g = gravitational acceleration: $g = 9.80$ m/s^2 in Brisbane QLD, Australia;
H = total head (m);
h = initial undershoot gate opening (m);
Q = water discharge (m^3/s);
S_f = friction slope: $S_f = -\partial H/\partial x$;
S_o = bed slope: $S_o = \sin\theta$;
t = time (s);
U = celerity (m/s) of negative surge leading edge for an observer standing on the bank positive upstream;
V = flow velocity positive downstream: $V = Q/A$;
V_x = instantaneous longitudinal velocity component (m/s);
x = longitudinal distance (m) positive downstream, with $x = 0$ at test section upstream end;
x_{Gate} = longitudinal coordinate (m) of the tainter gate (x_{Gate}11.15 m in this paper);
x_s = longitudinal coordinate (m) of negative surge leading edge;
z = vertical distance (m) positive upwards, with $z = 0$ at the bed;
θ = angle between channel bed and horizontal; and
ρ = water density (kg/m^3).

Subscripts

Gate = flow properties at tainter gate;
o = initial flow conditions, i.e., upstream of the negative surge leading edge; and
x = longitudinal direction positive downstream.

References

British Standard Institution. (1943). "Flow measurement." *BS 1042:1943*, British Standards, London.
Chanson, H. (2004). *Environmental hydraulics of open channel flows*, Elsevier-Butterworth-Heinemann, Oxford, UK.
Chanson, H. (2010). "Unsteady turbulence in tidal bores: Effects of bed roughness." *J. Waterway Port Coast. Ocean Eng.*, 136(5), 247–256.
Chanson, H., Trevethan, M., and Koch, C. (2007). "Discussion of 'Turbulence measurements with acoustic Doppler velocimeters'." *J. Hydraul. Eng.*, 133(11), 1283–1286.
Courant, R., Isaacson, E., and Rees, M. (1952). "On the solution of nonlinear hyperbolic differential equations by finite differences." *Commun. Pure Appl. Math.*, 5(3), 243–255.
Docherty, N. J., and Chanson, H. (2012). "Physical modeling of unsteady turbulence in breaking tidal bores." *J. Hydraul. Eng.*, 138(5), 412–419.
Favre, H. (1935). *Etude Théorique et Expérimentale des Ondes de Translation dans les Canaux Découverts (Theoretical and Experimental Study of Travelling Surges in Open Channels)*, Dunod, Paris (in French).
Flow-3D Version 9.2 [Computer software]. Flow Science Inc., Santa Fe, NM.
Goring, D. G., and Nikora, V. I. (2002). "Despiking acoustic Doppler velocimeter data." *J. Hydraul. Eng.*, 128(1), 117–126.
Henderson, F. M. (1966). *Open channel flow*, MacMillan, New York.
Jaeger, C. (1956). *Engineering fluid mechanics*, Blackie & Son, Glasgow, UK.
Koch, C., and Chanson, H. (2009). "Turbulence measurements in positive surges and bores." *J. Hydraul. Res.*, 47(1), 29–40.
Lauber, G. (1997). "Experimente zur Talsperrenbruchwelle im glatten geneigten Rechteckkanal (Dam break wave experiments in rectangular channels)." Ph.D. thesis, VAW-ETH, Zürich, Switzerland (in German).
Lauber, G., and Hager, W. H. (1998). "Experiments to dambreak wave: Horizontal channel." *J. Hydraul. Res.*, 36(3), 291–307.
Microsonic. (2012). "Online catalogue: mic+25/IU/TC." *Microsonic GMBH*, ⟨http://www.microsonic.de⟩ (Apr. 12, 2012).
Montes, J. S. (1998). *Hydraulics of open channel flow*, ASCE, New York.
Nortek. (2009). *Vectrino velocimeter user guide*, Nortek AS, Norway.
Reichstetter, M., and Chanson, H. (2011). "Physical and numerical modelling of negative surges in open channels." *Hydraulic Model Rep. No. CH84/11*, School of Civil Engineering, The Univ. of Queensland, Brisbane, Australia.
Sturm, T. W. (2001). *Open channel hydraulics, Water Resources and Environmental Engineering Series*, McGraw-Hill, Boston.
Tan, L., and Chu, V. H. (2009). "Lauber and Hager's dam-break wave data for numerical model validation." *J. Hydraul. Res.*, 47(4), 524–528.
Wahl, T. L. (2003). "Discussion of 'Despiking acoustic Doppler velocimeter data'." *J. Hydraul. Eng.*, 129(6), 484–487.